



Characterization of LC sensor structures realized by PCB and LTCC technology for determining moisture in building materials

Milan R. Radovanović*, Sanja P. Kojić, Dragana Z. Vasiljević, Goran M. Stojanović

Faculty of Technical Sciences, University of Novi Sad, Novi Sad, Serbia

Received 15 March 2017; Received in revised form 25 October 2017; Received in revised form 24 January 2018;
Accepted 10 February 2018

Abstract

This paper compares performances of two wireless sensors for measuring water concentration in building materials, one manufactured by the printed circuit board (PCB) technology and another one using the low temperature co-fired ceramics (LTCC) process. The fabricated sensors consist of inductive part (L) and interdigitated capacitive part (C) in one metal layer, connected in parallel. Inductance of inductive part was kept constant, whereas capacitance of capacitive part was changed by exposing the sensor to different moisture concentration, changing its resonant frequency. The variation of resonant frequency as a function of different water concentration was measured, using antenna coil and impedance analyser, in two widely used construction materials: clay brick and autoclaved aerated concrete block. Surface analysis for two sensors was performed by means of 3D profilometer. Mechanical properties of the sensors were measured for both conductive segments (copper and silver) and substrates materials (PCB and ceramics substrates) using nanoindenter. Comparative characteristics of the sensors are presented from their application point of view.

Keywords: LC sensor, nanoindenter, 3D profile, moisture

I. Introduction

Moisture in building materials represents a significant topic for our society. Water diffusion in porous building materials can result in the increased moisture concentration. The rise of moisture content in buildings can lead to many negative effects such as degradation of materials due to corrosion, disintegration of inorganic binders, frost action, bad hygienic conditions of interior climate, harmful microbial growth affecting human health, etc. [1]. Many historic buildings are threatened by increased harmful moisture contents. Monitoring of moisture content provides data for adequate decisions about reconstruction work. Furthermore, long term operation for industrial facilities where concrete structures play a vital role in the safety implies a necessity for complete monitoring system, including measuring water content in concrete [2] and concrete structures [3]. Therefore, methods for monitoring and measurement of percentage of moisture in building materials are very significant not only for researchers, but for wider community.

A technique for measuring the moisture content of masonry and cementitious materials can be to drill a hole in the material, collect the drilled material and perform measurement of its moisture by determining sample mass after and before drying [4]. However, this process is extremely low-speed and this technique is destructive. The development of portable nuclear magnetic resonance (NMR) system was investigated by Roels *et al.* [5] and could lead to surface moisture measurements. Various systems have been reported to give comprehensive information on the moisture content of building materials using the radiation attenuation approach. These can include X-ray systems [6], γ -ray systems [7] and neutron radiography [8], but these systems require a suitable radiation source and questions related to health and safety issues can be imposed. The dual-probe method is also one of suitable techniques for the measurement of moisture content [9], but in this method there are many potential sources of error. The time domain reflectometry (TDR) is sensitive to the presence of moisture and can be used for absolute measurements of the moisture content [10]. The practical applicability of TDR method was demonstrated on the measurement

*Corresponding author: tel: +381 21 485 2604,
e-mail: rmilan@uns.ac.rs

of moisture profiles in rod-shaped specimen of cellular concrete [11]. Suchorab [12] built three experimental model walls (autoclaved aerated concrete, red ceramic brick and silicate brick) and exposed them to moisture influence. TDR sensors were used for monitoring water uptake, based on the determination of electromagnetic pulse propagation speed in rods inserted into the studied material. Platt *et al.* [13] presented application of a non-invasive TDR sensor to image and parameterize the moisture content of base course materials which can be used for road construction.

Measurements of electrical parameters (L , C , Z) as well as the dielectric constant of porous materials are influenced by the moisture content and can be used for moisture content assessment. Commercial microwave moisture meters for measuring the dielectric constant of the medium in contact with the instrument are available and can evaluate the moisture content to a depth of 50 mm into a material [14]. Design, construction and experimental validation of moisture content sensors for building materials based on measuring conductivity was described by Guizzardi *et al.* [15]. However, this technique requires special samples of brick and wet applied mortars to be created, which is time and money consuming. The application of electromagnetic waves for monitoring concrete blocks' moisture level was presented by Kot *et al.* [16]. They used a microwave sensor operating in the frequency range from 2 to 6 GHz using a vector network analyser. The sensor frame presented in that paper has very complicated structure with three displacement transducers attached, with temperature sensor, etc. The application of microwave sensors to detect the 3D moisture profile within the wall was presented by Penirschke and Jakoby [17]. A small borehole with a diameter of 8 mm should be drilled into the wall to insert a coaxial probe. From the variation of the effective dielectric constant of reflected signal, the moisture content can be determined.

The evaluation of measurement techniques for moisture content in three types of building stone specimens, using LC resonant sensors, was presented by Zhao *et al.* [18]. However, in these sensors two stainless steel bars acted as a capacitor and a coil inductor was constructed by wire wound on a PVC pipe, which is not practical approach and cannot be serially manufactured. The application of a wireless, passive LC sensor for real-time monitoring of water content in construction materials such as sands, subgrade soils, and concrete materials was reported [19]. However, the design of the sensor has overpass wire (in additional layer) for connection of inductive and capacitive part of the sensor which is not sophisticated solution and can cause problem in practical placement of the sensor element.

A microelectromechanical (MEMS) based system for monitoring the moisture level and temperature in concrete structures was developed [20], using complicated and costly microcantilever beams and moisture-sensitive thin polymer. There has been considerable re-

cent interest in the mechanical characterization of bulk materials or thin films [21] using depth-sensing indentation tests with different shape of indenters. Indentation at nano-scale (or nanoindentation) has the advantages of being simple, cheap, reproducible, and relatively non-destructive method. Nanoindentation tests have been reported as very powerful methods for measurement of the mechanical properties of substrates or metallic films [22,23], since they play a key role in microelectronic components.

This paper describes two types of sensors which are used for detection of the percentage of moisture in construction materials. One sensor was fabricated by extremely low-cost PCB technology, whereas another one was fabricated by LTCC technology enabling exposure to harsh environment. LTCC is a multi-layer technology, based on ceramic substrate, which is co-fired with low resistance metal conductors (for example Ag or Cu) at low firing temperatures (less than 1000 °C). The ceramic substrate is usually produced by mixing ceramic and glass powders of exact composition as well as small amount of binding agent and solvent. The sensors have been designed as LC structure in one metal layer, which is the most appropriate realization providing a good contact between sensor and construction material under test. We successfully tested these sensors, measuring moisture in clay brick and autoclaved aerated concrete block. Performances of these sensors have been compared using impedance spectroscopy, surface analysis and characterization of their mechanical performances.

II. Experimental

2.1. Sensors design and manufacturing

Design of the sensors has been dictated with the following conditions: i) it should be passive LC sensors – enabling functioning without battery; ii) it should be fabricated in one metal layer (without wires for underpass or overpass) – enabling a good adhesion/contact of the sensor and construction materials under test; iii) one sensor should be manufactured by cost-effective PCB technology and another one by robust LTCC technology – enabling exposure of these sensors to harsh environment (moisture, temperature, corrosion, radiation, etc.); iv) the application of these sensors should be simple and flexible – enabling application both during construction of buildings and in later repair processes (if it is necessary).

Following above-mentioned guidelines and using our previous expertise in optimal design of inductors, we suggested “smart” design of a sensor with one metal layer of inductive part and capacitive part as interdigitated electrode structure. Figure 1a shows LC sensor manufactured by PCB technology. The sensor resonant circuit was created of a planar inductor and interdigital capacitor on a printed circuit board (PCB), known as FR-4. The printed circuit pattern was created by a “subtractive” process. In the subtractive process, the en-

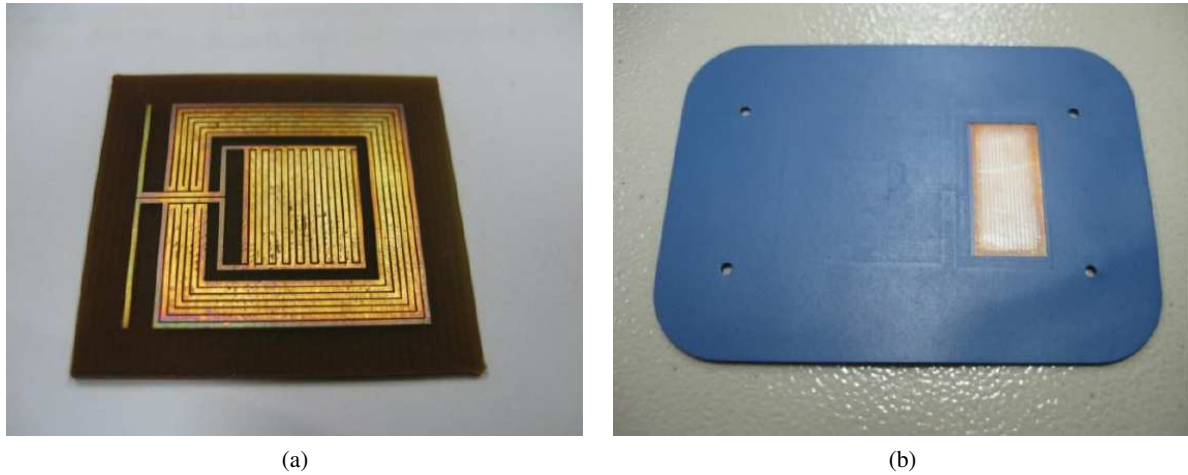


Figure 1. PCB (a) and LTCC (b) sensor

tire surface of the substrate is first plated using copper, and then the areas that are not part of the desired pattern (L and C) are chemically etched away, or subtracted. The sensor manufactured by LTCC technology consists of ceramic Heraeus CT700 substrate layer and silver as a conductive layer. The obtained multilayer structure was co-fired in a six-zones belt furnace at a maximum temperature of 880 °C and a firing process time of 2 h. Figure 1b shows LTCC sensor where inductive part is not obviously visible, because it is covered by dielectric layer (Heraeus CT700 dielectric tape). Dimensions of the presented sensors are given in Tables 1 and 2 for inductor and capacitor, respectively.

The profiles of the fabricated sensors (i.e. thicknesses of the copper and silver lines) were analysed by non-contact measurement using profilometer Huvitz HRM 300. 2D profiles of both sensors are shown in Fig. 2. To decrease the effect of surface roughness, the measured values are averaged on x - and y -axes. 3D images were also obtained (Fig. 2) from 50 measurements of 2D profiles and applying image processing protocol and their combination in one 3D model. The samples profile

Table 1. Parameters chosen for the planar inductor

Parameter	PCB	LTCC
Coil geometry	atypical square	atypical square
Length of side [mm]	46	18.4
Number of turns	7	13
Width of metal line [mm]	1	0.4
Space between turns [mm]	0.2	0.08
Metal layer thickness [mm]	0.034	0.01

Table 2. Parameters chosen for the interdigitated capacitor

Parameter	PCB	LTCC
Finger width [mm]	1	0.4
Spacing between fingers [mm]	0.2	0.08
Overlap length between fingers [mm]	23.4	16.72
Metalization thickness [mm]	0.034	0.01
Total number of fingers	18	18

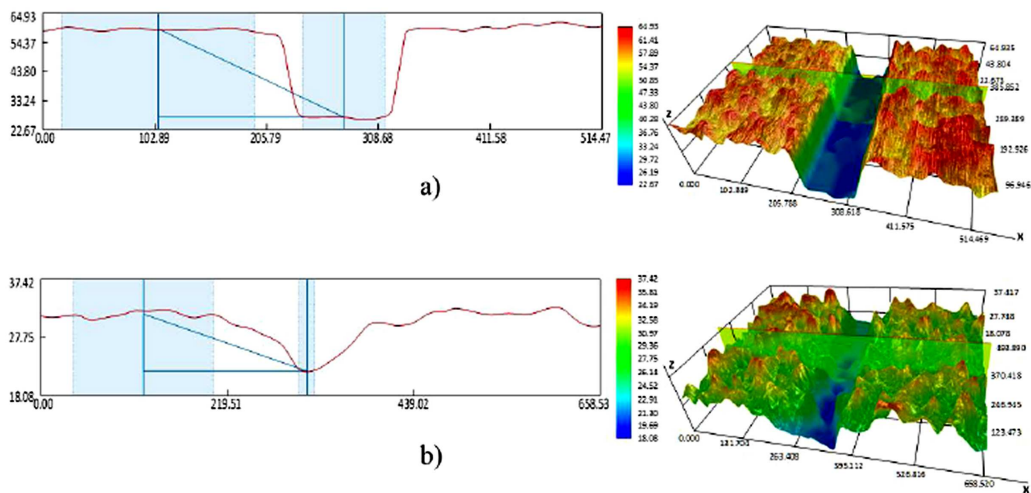


Figure 2. 2D and 3D profiles of: a) PCB and b) LTCC sensor (units are in μm)

lines are averaged arrays of values collected from the same x-axes values and selected y-range around the profile measurement lines. The obtained thickness of PCB electrodes is around $31.8\ \mu\text{m}$ and for LTCC electrodes $9.5\ \mu\text{m}$, that are very close to the chosen parameters given in Tables 1 and 2.

2.2. Working principles

Working principle of the presented sensors is based on the capacitance change of sensor's capacitive part when it is exposed to different moisture concentration (similar principle was already reported in our earlier papers [24,25]). Namely, dielectric constant of water is greater than for the air, thus capacitance increases with increasing the water content in tested building materials. In that way, resonant frequency (given by Eq. 1) of the LC sensor decreases and this variation can be detected using antenna coil connected to an impedance analyser or to a hand held microcontroller based device.

$$f_{res} = \frac{1}{2\pi\sqrt{L \cdot C}} \quad (1)$$

In Eq. 1 f_{res} is resonant frequency of the LC circuit, whereas L and C are inductance and capacitance of inductive and capacitive part of the sensor structure, respectively.

2.3. Testing procedure

Two widely used construction materials: i) clay brick ($250 \times 120 \times 65\ \text{mm}$) and ii) autoclaved aerated concrete block ($230 \times 200 \times 100\ \text{mm}$) were used to test the proposed sensors. These construction materials were immersed into a container with water and brick and concrete block capillary absorbed water/moisture up to saturation. Afterwards, during drying process, measurement of the brick and concrete block weights was conducted as well as the measurement of sensor resonant frequency (in some time intervals) by means of HP4194A impedance analyser. It is important to underline that creation of water chains was not observed during the sensors testing, suggesting that shortening between capacitor fingers did not happen. The experimental set-up is shown in Fig. 3.

The fabricated sensors are intended to be used in harsh environment and they have to handle different mechanical stresses. Because of that the mechanical performances of the sensors were also studied. Mechanical properties (load-displacement curves, elastic modulus and hardness) of the sensors were measured for both conductive segments (copper and silver) and substrates materials (PCB substrate and ceramics), using Nanoindenter Agilent G200 with the three-sided Berkovich type of indenter. Ten measurements per sample on different locations as a function of displacement into the surface were performed. The forces involved were up to $100\ \text{mN}$ with a resolution of a $50\ \text{nN}$. The depths of penetration were on the order of microns with a resolution of less than a nanometre.

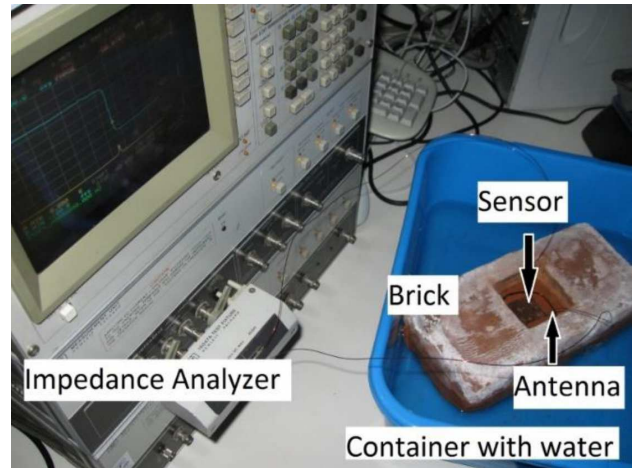


Figure 3. Experimental setup for measuring water content in building material using LC wireless sensors

III. Results and discussion

3.1. Variation of resonant frequency

In subsection 2.2 it was already discussed that, according to the theory and working principles, capacitance is greater with the increase in the percentage of moisture and accordingly the resonant frequency of LC sensors decrease. This was confirmed by measuring resonant frequency using the developed sensors in two construction materials: clay brick and autoclaved aerated concrete block, as can be seen in Figs. 4 and 5, respectively. The measurements showed that clay brick can absorb moisture up to 18% of its weight, whereas autoclaved aerated concrete block absorbs up to 60%. This is in agreement with the internal structure of these materials. Clay brick has dense internal structure and autoclaved block has more porous structure with the average pore sizes around $800\ \mu\text{m}$ (Fig. 6). This structure provides possibility for autoclaved block to absorb more moisture, but also it can be dried faster compared to classical clay brick. On the other hand, the clay

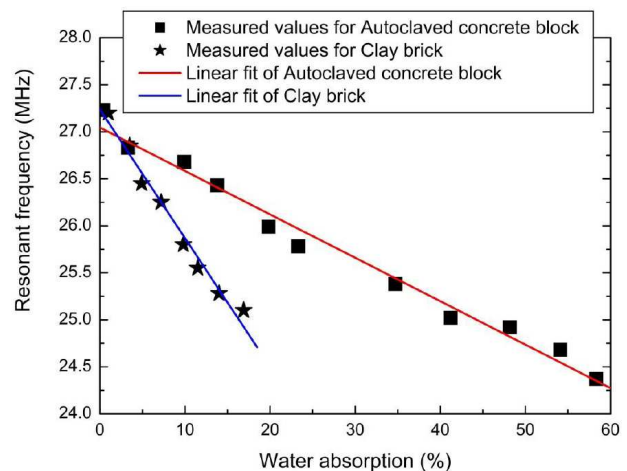


Figure 4. Variation of resonant frequency as a function of water concentration in autoclaved aerated concrete block and clay brick, for PCB sensor

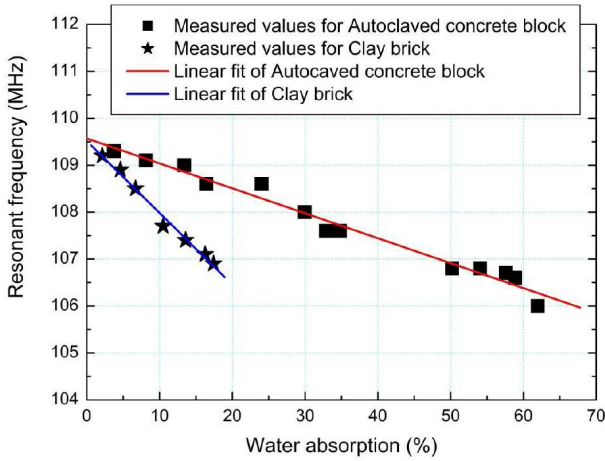
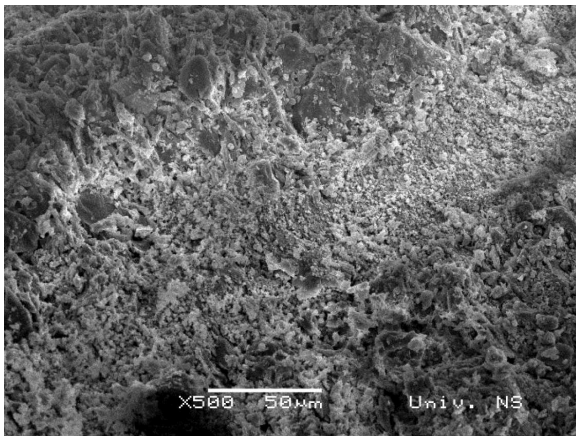


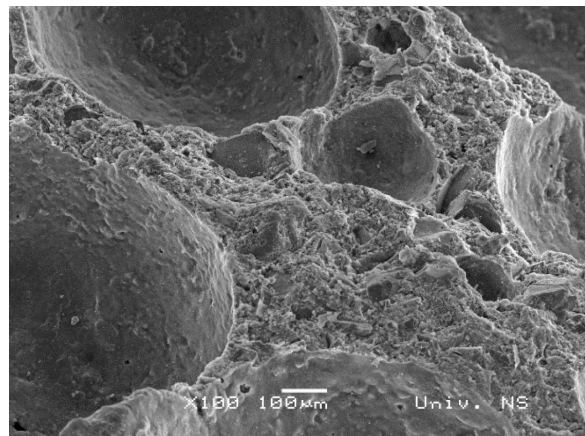
Figure 5. Variation of resonant frequency as a function of water concentration in autoclaved aerated concrete block and clay brick, for LTCC sensor

brick internal structure enables better adhesion/contact of the sensor(s) with the surface of the analysed samples, which consequently results in better sensitivity for this sample. Table 3 summarizes the sensitivity data for PCB and LTCC sensors.

From Table 3 and already presented dimensions (Tables 1 and 2) it can be concluded that the highest sensitivity has been shown for the LTCC sensor applied in the clay brick. This can be explained by the fact that this sensor has spacing between fingers equal to 80 μm and in that way it is possible to reach higher capacitance as well as the range of capacitance and consequently resonant frequency variation. The PCB sensor had spacing among fingers of interdigitated capacitor equal to 100 μm, which is the limit of the applied technological process.



(a)



(b)

Figure 6. SEM micrographs, (a) clay brick, (b) autoclaved aerated concrete block

Table 3. Active area of sensor (sensitive layer) and sensitivity of the proposed sensors

Sensor type	Active sensor area [mm ²]	Sensitivity of sensor in clay brick	Sensitivity of sensor in autoclaved aerated concrete block
PCB sensor	655.36	0.1324 MHz/1%	0.0538 MHz/1%
LTCC sensor	338.56	0.1483 MHz/1%	0.0550 MHz/1%

3.2. Mechanical characterization

Typical load-displacement curves have four segments (which can be also seen in Figs. 7 and 8): i) the loading segment; ii) the holding segment at maximum load (only 1 second); iii) the unloading segment and recovery period. Loading curves obtained with Berkovich indenters can be simply described by the relation $P = C \cdot h^n$ where P is the indentation load, h is the measured depth, C is a material constant and the derived exponent n is less than 2, both related to the elastic and plastic properties of the material.

It can be seen from Fig. 7 that the hysteresis provided by loading-unloading curves for the LTCC substrate is smaller than for PCB ones, indicating that LTCC substrate has higher elasticity (which can be expressed by the Young modules) than PCB substrate. The loading curves have higher slope for harder material, such as in the case of LTCC substrate than the PCB substrate (hardness of these materials given in Table 4 confirms the same). Moreover, the unloading curves are close to straight vertical line if the material shows more plastic behaviour such as for the PCB substrate. In almost all curves depicted in Figs. 7 and 8, a viscoelastic return of the samples after the hold load periods can be seen. This recovery period is more obvious in LTCC substrate and it is around 1600 nm for LTCC substrate and approximately 4550 nm in PCB substrate (Fig. 7).

It can be concluded that with the same load, for example at the maximum of 100 mN, penetration into LTCC ceramic substrate was around 2800 nm, whereas the depth of penetration of the indenter into the PCB substrate surface was approximately 5000 nm.

From loading part of the load-displacement curve from Fig. 7, it can be seen that humid substrates' (both PCB and LTCC) curves have higher slope than for

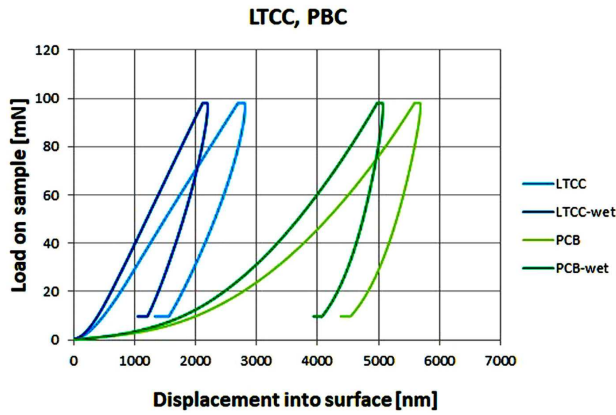


Figure 7. Average curves of applied load as a function of displacement into LTCC and PCB substrates

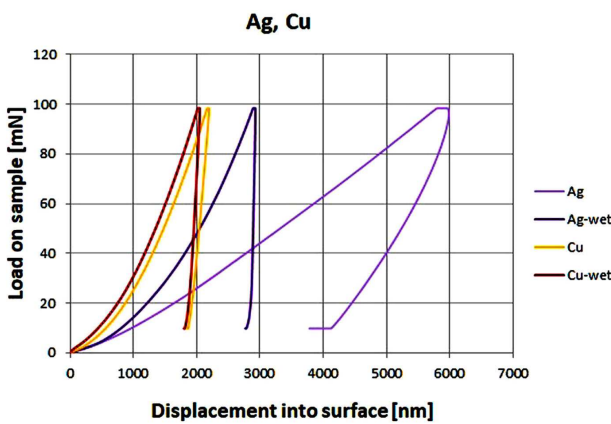


Figure 8. Average curves of applied load as a function of displacement into Cu and Ag conductive layers

the dry substrates indicating higher elasticity and also higher value of Young's module, which is also visible from Table 4. This is a result of water penetration into PCB internal structure, making it softer and with higher elasticity, because FR-4 woven fiberglass cloth becomes softer and epoxy resin is not any more such a strong binder. Typical LTCC microstructure has closed pores and absorption (or passing) of the water in the substrate is difficult, thus the moisture remains in the surface area. Measurements show that this surface area is thicker than 2000–2500 nm causing LTCC curve to shift to the left as well as for PCB curve.

Moreover, we performed also mechanical characterization of conductive segments of the analysed sensors;

Table 4. Values (mean value and standard deviation) of Young's modulus and hardness for LTCC and PCB substrates as well as for Ag and Cu conductive segments

Materials type	Dry environment		In wet medium (100% of humidity)	
	Young's modulus [GPa]	Hardness [GPa]	Young's modulus [GPa]	Hardness [GPa]
Heraeus CT700 – LTCC substrate	11.28 (3.79) ^a	0.644 (0.090)	11.03 (2.04)	0.582 (0.169)
FR-4 – PCB substrate	8.32 (3.20)	0.037 (0.004)	2.77 (0.64)	0.049 (0.007)
Ag – LTCC conductive segments	9.33 (4.75)	0.319 (0.059)	2.10 (0.97)	0.064 (0.020)
Cu – PCB conductive segments	18.51 (4.03)	0.837 (0.186)	0.0438 (0.159)	0.056 (0.019)

^avalues in brackets are standard deviation

more precisely, the test was conducted on copper/silver segments of interdigitated capacitive structure. Figure 8 presents average curves of load applied on Ag and Cu layers as a function of displacement. It can be concluded that at the same force of 310 mN penetration into silver layer (LTCC sensor) was around 7000 nm, whereas penetration into Cu layer (PCB sensor) was around 4000 nm. It can be seen that penetration of the Berkovich tip is about 18% of the total thickness of Cu, while the penetration of the Ag layer is about 21% of the total layer thickness. Figure 8 also reveals that both conductive materials become harder when they are exposed to water environment and penetration is shallower.

Table 4 presents values of Young's modulus (elastic modulus) and indentation hardness for LTCC and PCB substrates as well as for Ag and Cu conductive segments of both sensors (because information from data sheets for separate materials cannot be treated as valid for manufactured component, such as the sensor in our case). Hardness is important since it is related to the strength or fracture toughness of the proposed sensors, whereas elastic modulus provides a measure of their stiffness or compliance. From experimental results we can conclude that LTCC substrate (Heraeus CT700 ceramic tape) has higher hardness than standard FR-4 material for PCB substrate. Furthermore, silver as a conductive material for LTCC sensors has better elasticity and greater hardness in comparison with copper as a conductive material for PCB sensor. For mechanical characterization samples were soaked into the ionised water for 24 h before mechanical measurements and for electrical characterization humidity exposure was done during the measurements.

Mechanical characterization of the presented sensors was performed on fabricated components, which were used in practical applications for measuring water content in building materials. That means nanoindentation tests were not conducted immediately after fabrication, but after usage of these sensors to measure different percentage of humidity. In that context, it can be said that our results include ageing effects on the mechanical performances of the fabricated sensors (components), and not characterization of separate layers (as it is usually done in open literature). Also Ag and Cu layers are not chemically pure Ag and Cu elements. They have surfactants and additives that make them usable for fabrication techniques. This is explanation why there is some dis-

crepancies between the results presented in this paper (Table 4) and results presented in literature. For illustration, for Cu layer with 1 μm thickness, authors reported [22] hardness value of 1.7 GPa and elastic modulus of 113 GPa and values in our paper are 0.837 and 18.5 GPa, respectively (but also for the total layer thickness of around 17 μm). Similarly, for silver layer the reported values in [23] are 0.2 GPa (for hardness) and 63 GPa (for elastic modulus), whereas in our paper these values are 0.319 and 9.3 GPa.

Some of the presented values in Table 4, have a relatively high standard deviation which is a consequence of the nanoindentation measurement on the surface which is not ideally flat (see profile in Fig. 2). Also, some of the analysed sensor structures have already been used for monitoring moisture in buildings. Furthermore, several layers (e.g. Ag conductive layer) were oxidized to some extent and this has had influence on the standard deviation of presented measuring results.

IV. Conclusions

In this paper two types of LC sensors for monitoring moisture in construction materials have been presented and comparative analysis of their characteristics was performed. One sensor was fabricated by PCB technology, whereas the other one in LTCC technology. These sensors have been successfully applied for detection of water content in the clay brick and autoclaved aerated concrete block. The nanoindentation tests have provided valuable information on the elastic modulus, hardness and load-displacement curve for both sensors. The differences in the manufacturing processes determined that LTCC sensor can be exposed to harsh environment, can handle higher range of temperature and has higher values of Young's module and hardness, compared to the PCB substrate. PCB sensors are inexpensive and their behaviour is acceptable for intended application.

Acknowledgement: This work is supported by the Ministry of education, science and technological development in the framework of the project no. TR32016 and III45021 as well as project no. 142-451-2484/2017-01/01 financed by the Provincial secretariat for higher education and R&D.

References

1. J.C. Morel, A. Pkla, P. Walker, "Compressive strength testing of compressed earth blocks", *Constr. Build. Mater.*, **21** (2007) 303–309.
2. A. Courtois, F. Taillade, G. Moreau, T. Clauzon, F. Skoczylas, B. Masson, "Water content monitoring for nuclear concrete buildings: needs, feedback and perspectives", *Poromechanics V: Proceedings of the Fifth Biot Conference on Poromechanics*, (2013) 1654–1663.
3. W. John McCarter, Ø. Vennesland, "Sensor systems for use in reinforced concrete structures", *Constr. Build. Mater.*, **18** (2004) 351–358.
4. M.C. Phillipson, P.H. Baker, M. Davies, Z. Ye, A. McNaughtan, G.H. Galbraith, R.C. McLean, "Moisture measurement in building materials: An overview of current methods and new approaches", *Build. Serv. Eng. Res. Technol.*, **28** (2007) 303–316.
5. S. Roels, J. Carmeliet, H. Hens, O. Adan, H. Brocken, R. Cerny, Z. Pavlik, A.T. Ellis, C. Hall, K. Kumaran, L. Pel, R. Plagge, "A comparison of different techniques to quantify moisture content profiles in porous building materials", *J. Thermal Env. Bldg. Sci.*, **27** (2004) 261–276.
6. V. Cnuddea, J.P. Cnuddea, C. Dupuisb, P.J.S. Jacobs, "X-ray micro-CT used for the localization of water repellents and consolidants inside natural building stones", *Mater. Character.*, **53** (2004) 259–271.
7. R. Wormald, A.L. Britch, "Methods of measuring moisture content applicable to building materials", *Build. Sci.*, **3** (1969) 135–145.
8. H. Justnes, K. Bryhn-Ingebrigtsen, G.O. Rosvold, "Neutron radiography: an excellent method of measuring water penetration and moisture distribution in cementitious materials", *Adv. Cement Res.*, **6** (1994) 67–72.
9. M. Davies, M. Tirovic, Z. Ye, P.H. Baker, "A low cost, accurate instrument to measure the moisture content of building envelopes in-situ: a modelling study", *Build. Serv. Eng. Res. Technol.*, **25** (2004) 295–304.
10. M.C. Phillipson, P.H. Baker, M. Davies, Z. Ye, G.H. Galbraith, R.C. McLean, "Suitability of time domain reflectometry for monitoring moisture in building materials", *Build. Serv. Eng. Res. Technol.*, **29** (2008) 261–272.
11. L. Fiala, M. Pavlíková, Z. Pavlík, "Application of TDR method for moisture profiles measurement in cellular concrete", *Adv. Mater. Res.*, **982** (2014) 11–15.
12. Z. Suchorab, "Noninvasive moisture measurement in building materials", pp. 433–439 in *Environmental Engineering IV – Pawłowski, Dudzinska & Pawłowski (eds)*, Taylor & Francis Group, London, 2013.
13. I. Platt, I. Woodhead, P. Harrington, A.E.C. Tan, "Imaging and parameterizing moisture in road sub course using time domain reflectometry", *IEEE Sensors J.*, **16** (2016) 4760–4766.
14. M.J. Dill, "A review of testing for moisture in building elements", *Construction Industry Research and Information Association*, London, 2000.
15. M. Guizzardi, D. Derome, D. Mannes, R. Vonbank, J. Carmeliet, "Electrical conductivity sensors for water penetration monitoring in building masonry materials", *Mater. Struct.*, **49** (2016) 2535–2547.
16. P. Kot, A. Shaw, K.O. Jones, J.D. Cullen, A. Mason, A.I. Al-Shamma'a, "The feasibility of electromagnetic waves in determining the moisture content of concrete blocks", pp. 251–256 in *Ninth International Conference on Sensing Technology*, 2015.
17. A. Penirschke, R. Jakoby, "Metamaterial transmission line resonators for structural moisture sensing in buildings", *IEEE Instrumentation and Measurement Technology Conference*, 2013.
18. J.H. Zhao, E. Rivera, A. Mufti, D. Stephenson, D.J. Thomson, "Evaluation of dielectric based and other methods for moisture content measurement in building stones", *J. Civil Struct. Health Monit.*, **2** (2012) 137–148.
19. J.B. Ong, Z. You, J. Mills-Beale, E.L. Tan, B.D. Pereles, K.G. Ong, "A wireless, passive embedded sensor for real-time monitoring of water content in civil engineering materials", *IEEE Sensors J.*, **8** (2008) 2053–2058.

20. A. Norris, M. Saafi, P. Romine, “Temperature and moisture monitoring in concrete structures using embedded nanotechnology/microelectromechanical systems (MEMS) sensors”, *Constr. Build. Mater.*, **22** (2008) 111–120.
21. Z. Chen, X. Wang, N. Brandon, A. Atkinson, “Analysis of spherical indentation of porous ceramic films”, *J. Eur. Ceram. Soc.*, **37** (2017) 1031–1038.
22. Z.H. Cao, P.Y. Li, H.M. Lu, Y.L. Huang, X.K. Meng, “Thickness and grain size dependent mechanical properties of Cu films studied by nanoindentation tests”, *J. Phys. D: Appl. Phys.*, **42** (2009) 065405.
23. S. Cherneva, R. Iankov, D. Stoychev, “Characterisation of mechanical properties of electrochemically deposited thin silver layers”, *Transactions IMF*, **88** [4] (2010) 209–214.
24. G. Stojanović, M. Radovanović, M. Malešev, V. Radonjanin, “Monitoring of water content in building materials using a wireless passive sensor”, *Sensors*, **10** [5] (2010) 4270–4280.
25. M. Maksimović, G. Stojanović, M. Radovanović, M. Malešev, V. Radonjanin, G. Radosavljević, W. Smetana, “Application of a LTCC sensor for measuring moisture content of building materials”, *Constr. Build. Mater.*, **26** [1] (2011) 327–333.